Analysis of the external filtered modes of a semiconductor laser with filtered optical feedback

Kirk Green[a] and Bernd Krauskopf[b]

[a]Department of Theoretical Physics, FEW, Vrije Universiteit, De Boelelaan 1081, 1081HV Amsterdam, The Netherlands

[b]Department of Engineering Mathematics, University of Bristol, Bristol BS8 1TR, UK

ABSTRACT

We present a detailed analysis of the external filter mode (EFM) structure of a semiconductor laser subject to filtered optical feedback (FOF). These EFMs form the 'backbone' of the dynamics of the system. Specifically, from the governing delay differential equations, we find analytic, transcendental expressions for both the solution curves, which define the frequency and amplitude of the EFMs, and their envelopes. We use numerical continuation to find and follow solutions of these equations. This approach allows us to show how the structure depends on the key parameters of filter width, filter detuning, and feedback phase. In other words, we identify the external influence of the filter on an otherwise fixed laser.

Keywords: Semiconductor lasers, filtered optical feedback (FOF), external filtered modes (EFM), EFM-components

1. INTRODUCTION

In this paper we investigate a semiconductor laser receiving filtered optical feedback (FOF) from an external mirror [1]. As its name suggests, in contrast to conventional optical feedback (COF), the FOF laser's light is subject to some filtering within the external cavity. This filtering may be due to, for example, vapour cells within the external cavity, or reflections from a diffraction grating that serves as the external mirror. FOF provides a way of controlling the laser's output. It can be used to provide single-mode operation, or to select certain frequencies of the laser light. Consequently, an investigation of the effect of a varying filter on the mode structure of the FOF laser is important.

We consider a delay differential equation (DDE) model describing a semiconductor laser subject to FOF [2] to show how the external filtered mode (EFM) structure of the FOF laser depends on the key parameters of filter width, filter detuning, and feedback phase. In particular, we show how the parameter-plane of filter width versus filter detuning is divided into regions in which the EFMs travel over a single or over two separate EFM-components. The boundary between these regions is given by transitions through extrema and saddles (in the surface of EFMs); the vertices of this region are identified as cusp points. Analytic expressions for these transitions are derived. In fact, the EFM-components can be described by a degree-four polynomial function of the filter parameters. Our analysis expands on previous results by presenting a global picture of the FOF laser's mode structure. Finally, in order to compare with results from COF, we illustrate the transition from one to two EFM-components in the mode frequency versus inversion plane.

E-mail addresses: k.green@few.vu.nl, b.krauskopf@bristol.ac.uk

symbol	meaning	value
α	linewidth enhancement factor	5
T	ratio of carrier to photon lifetimes	100.0
P	pump parameter	3.5
τ	external cavity round-trip time	500.0
κ	feedback rate	0.02
C_p	feedback phase	0.0
Λ	filter width	0.007
Δ	filter detuning	0.0, 0.0525, 0.0595 and 0.10222
Ω	detuning of laser w.r.t. reference	0.0

Table 1. Laser parameters.

2. RATE EQUATIONS

A single-mode semiconductor laser subject to FOF can be described by the dimensionless rate equations

$$\frac{dE}{dt} = (1+i\alpha)N(t)E(t) + \kappa F(t,\tau), \tag{1}$$

$$T\frac{dN}{dt} = P - N(t) - (1+2N(t))|E(t)|^2, \tag{2}$$

for the evolution of the slowly varying complex electric field $E(t) = E_x(t) + iE_y(t)$ and the population inversion $N(t)$. The parameter values we use are given in Table 1; see Ref. [1] for the full physical model.

The feedback term $\kappa F(t,\tau)$ in Eq. (1) involves the feedback rate κ and the round-trip time τ between the laser and the external mirror. We fix $\tau = 500$, corresponding to a distance between the laser and the external mirror of $L_{\text{ext}} \approx 21\,\text{cm}$.

If the light in the external cavity is not filtered then the feedback term in Eq. (1) can be written as $F(t,\tau) = E(t-\tau)$ (under the assumption of weak feedback). This is known as the Lang-Kobayashi model [3], and has received considerable attention.

Filtered optical feedback can be described using a single-Lorentzian approximation as

$$F(t,\tau) = \Lambda e^{i(C_p - \Omega\tau)} \int_{-\infty}^{t} E(s-\tau) \exp\left[(i(\Delta-\Omega)-\Lambda)\,(t-s)\right] ds\,, \tag{3}$$

where the parameter Λ describes the filter width, Δ describes the filter detuning (with respect to the free-running, fixed laser) and C_p describes the feedback phase of the external round-trip. Furthermore, we write the equations in the frame of reference of a fixed solitary laser, and introduce Ω to measure the detuning of the laser, for example, due to changes in experimental conditions, with respect to the fixed laser's frequency. In the numerical examples that follow, we will consider $\Omega = 0$. In other words, the laser parameters are kept fixed at all times. We consider the effect of changes in the filtered field, which is fed back into the laser, that is, we consider the parameters Λ, Δ and C_p.

Differentiating Eq. (3), with respect to time, leads to the following differential equation

$$\frac{dF}{dt} = \Lambda E(t-\tau) e^{i(C_p - \Omega\tau)} + (i(\Delta-\Omega)-\Lambda)\,F(t) \tag{4}$$

for the complex feedback field $F(t) = F_x(t) + iF_y(t)$. Note that in Eq. (4), as $\Lambda \to \infty$, we recover the equation for COF because $F(t,\tau) \to E(t-\tau)$.

The semiconductor laser subject to FOF is described by Eqs. (1), (2) and (4). Like the Lang-Kobayashi equations describing the COF laser, these FOF laser equations have S^1-symmetry under the transformation $(E,N,F) \to (cE,N,cF)$, where $\{c \in \mathbb{C} : |c| = 1\}$. In other words, rotating any solution in the complex E and F planes over any angle $b \in [0, 2\pi]$ gives another solution of Eqs. (1), (2) and (4).

Finally, we remark that Eqs. (1), (2) and (4) are extremely similar in structure to the equations describing non-instantaneous phase-conjugate feedback [4]. The interaction time within the phase-conjugating mirror plays a similar role to the inverse of the filter width of the FOF laser.

3. EXTERNAL FILTERED MODES

The basic steady state solutions of Eqs. (1), (2) and (4) are known as the *external filtered modes* (EFMs). They are given as

$$(E(t), N(t), F(t)) = (E_s e^{i(\omega_s - \Omega)t},\, N_s,\, F_s e^{i(\omega_s - \Omega)t + i\Phi}) \tag{5}$$

where $E_s, N_s, F_s, \omega_s, \Phi \in \mathbb{R}$. To find EFMs, one must first find an expression for their frequencies ω_s. This is done as follows.

Firstly, we substitute Eq. (5) into Eq. (1), and equate real and imaginary parts to give

$$0 = N_s E_s + \kappa F_s \cos\Phi, \tag{6}$$

$$E_s(\omega_s - \Omega) = \alpha N_s E_s + \kappa F_s \sin\Phi. \tag{7}$$

Upon elimination of N_s, this yields

$$\omega_s - \Omega = \kappa \frac{F_s}{E_s} \left[-\alpha \cos\Phi + \sin\Phi \right]. \tag{8}$$

Alternatively*, Eq. (8) can be written as

$$\omega_s - \Omega = \kappa \frac{F_s}{E_s} \sqrt{1+\alpha^2} \sin(\Phi - \arctan\alpha). \tag{9}$$

Next we substitute Eq. (5) into Eq. (4) to give

$$0 = \Lambda E_s \cos(C_p - \Phi - (\omega_s - \Omega)\tau) - \Lambda F_s, \tag{10}$$

$$F_s(\omega_s - \Omega) = \Lambda E_s \sin(C_p - \Phi - (\omega_s - \Omega)\tau) + \Delta F_s, \tag{11}$$

leading to the following two expressions for F_s/E_s:

$$\frac{F_s}{E_s} = \cos(C_p - \Phi - (\omega_s - \Omega)\tau) \tag{12}$$

and

$$\frac{F_s}{E_s} = -\frac{\Lambda}{\Delta - \omega_s} \sin(C_p - \Phi - (\omega_s - \Omega)\tau). \tag{13}$$

Moreover, Eq. (12) and Eq. (13) can be squared and added leading to

$$\frac{F_s}{E_s} = \pm \frac{\Lambda}{\sqrt{\Lambda^2 + (\Delta - \omega_s)^2}}. \tag{14}$$

The negative solution above can be neglected as $E_s \geq 0$ and $F_s \geq 0$. Furthermore, Eqs. (12) and (13), and the positive solution of Eq. (14) have been checked to give identical results.

Finally, substituting Eq. (14) into Eq. (8) results in the following equation for ω_s:

$$\Omega = \omega_s + \kappa\Lambda \sqrt{\frac{1+\alpha^2}{\Lambda^2 + (\Delta - \omega_s)^2}} \sin\left(-\Phi + \arctan\alpha\right) \tag{15}$$

where Φ is obtained from Eq. (12) and Eq. (13). Namely,

$$\Phi = C_p - (\omega_s - \Omega)\tau + \arctan\left(\frac{\Delta - \omega_s}{\Lambda}\right). \tag{16}$$

Using this expression for Φ, it can be seen that the argument of both the cos and sin terms of Eqs. (12) and (13) reduce to $\arctan\left(\frac{\Delta-\omega_s}{\Lambda}\right)$; thus, clearly showing their equivalence.

*Here we use $a\sin x + b\cos x = \sqrt{a^2+b^2}\sin(x+\phi)$ where $\tan\phi = b/a$.

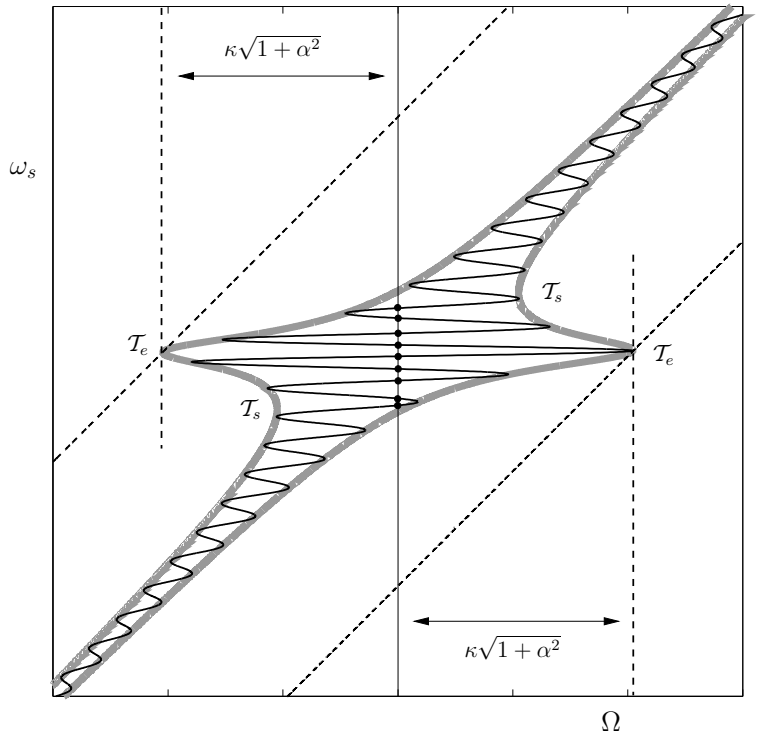

Figure 1. General solution curve (black) and its envelope (grey).

3.1. Solution curve and envelope

Equation (15) defines the *solution curve*. In other words, for fixed laser parameters κ and α, fixed filter parameters Δ, Λ and C_p and, in particular, for fixed Ω, the roots of Eq. (15) are the frequencies ω_s of the EFMs.

Figure 1 shows such a solution curve (in black) for the fixed parameters given in Table 1. The intersections of the black solution curve with a vertical line give the frequencies ω_s for a given Ω. In this case, the values of ω_s are shown as black dots for $\Omega = 0$.

As for the COF laser, from Eq. (16), it is clear that increasing the delay time τ increases the number of EFMs, while changing the feedback phase C_p over 2π traces the path from one EFM to the next (all other parameters assumed fixed). Moreover, Eq. (15) shows that varying Δ shifts the bulge of the solution curve along the diagonal $\Omega = \omega_s$ (the phase is also shifted with Δ; see Eq. (16)).

Furthermore, the solution curve is contained within a *solution envelope* (shown in grey in Fig. 1). The equation for this envelope is given by the maxima of Eq. (15). In other words, by $|\sin(-\Phi + \arctan\alpha)| = 1$. This gives

$$\Omega_e(\omega_s) = \omega_s \pm \kappa\Lambda\sqrt{\frac{1+\alpha^2}{\Lambda^2 + (\Delta - \omega_s)^2}}. \tag{17}$$

As the filter width $\Lambda \to \infty$ it is seen from Eq. (17) that

$$\Omega_e(\omega_s) \to \omega_s \pm \kappa\sqrt{1+\alpha^2}. \tag{18}$$

In other words, the solution envelope moves to the dashed lines of Fig. 1 and, hence, we recover the constant sinusoidal solution curve describing the external cavity modes (ECMs) of the COF laser.

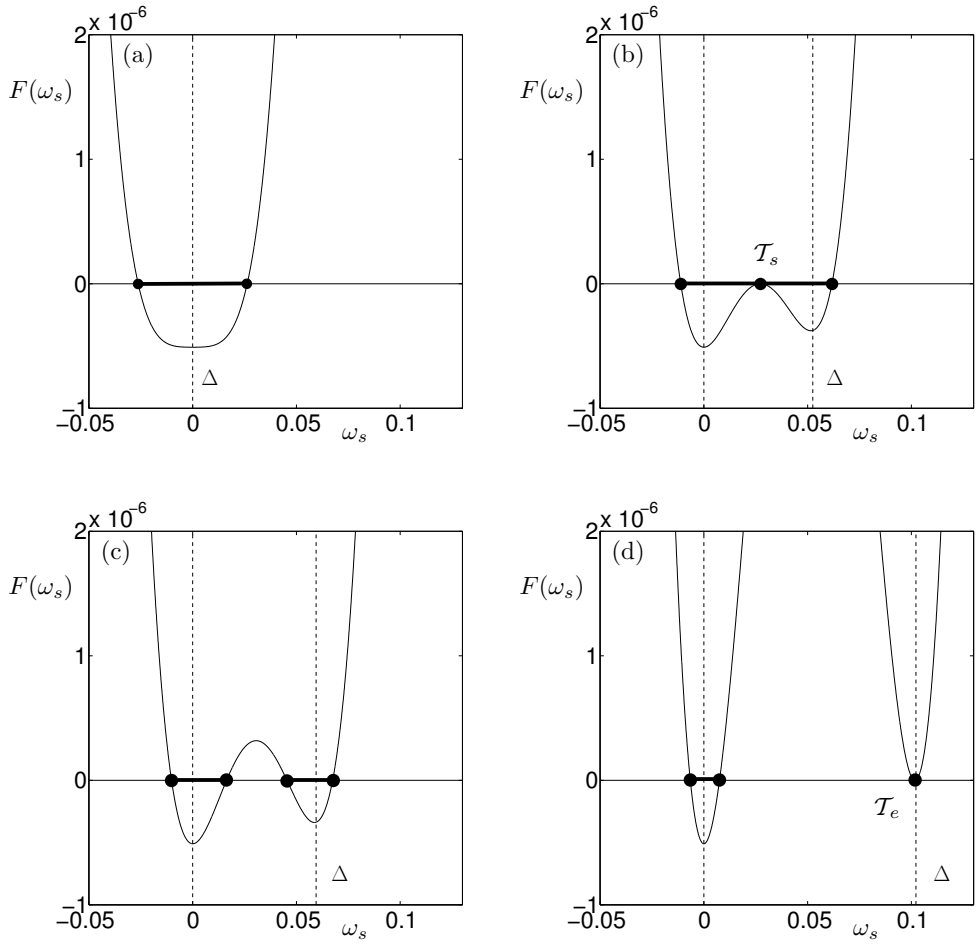

Figure 2. Fourth-order curve Eq. (21) for $\Delta = 0.0$ (a), 0.0525 (b), 0.0595 (c) and 0.10222 (d).

Lastly, we note that the shape of the solution envelope is independent of C_p; recall that varying C_p has the effect of shifting the position of the solution curve within this fixed envelope. The solution curve reaches the left extrema of the solution envelope for

$$C_p \quad = \quad \frac{\pi}{2} + \arctan\alpha + 2n\pi,\ n \in \mathbb{Z}, \tag{19}$$

and the right extrema for

$$C_p \quad = \quad \frac{\pi}{2} + \arctan\alpha + (2n+1)\pi,\ n \in \mathbb{Z}. \tag{20}$$

These values of C_p become very important when considering the so-called injection limit of the FOF laser $\Lambda \to 0$; see Ref. [1].

3.2. EFM-components

From here on, we consider solutions with $\Omega = 0$, that is, the laser parameters are kept fixed at all times. The detuning between laser and filter is given by Δ.

Equation (17) gives intersections of the envelope with $\Omega = 0$ as roots of the degree-four polynomial

$$F(\omega_s) = \omega_s^2 \left((\Delta - \omega_s)^2 + \Lambda^2 \right) - \kappa^2 \Lambda^2 \left(1 + \alpha^2 \right). \tag{21}$$

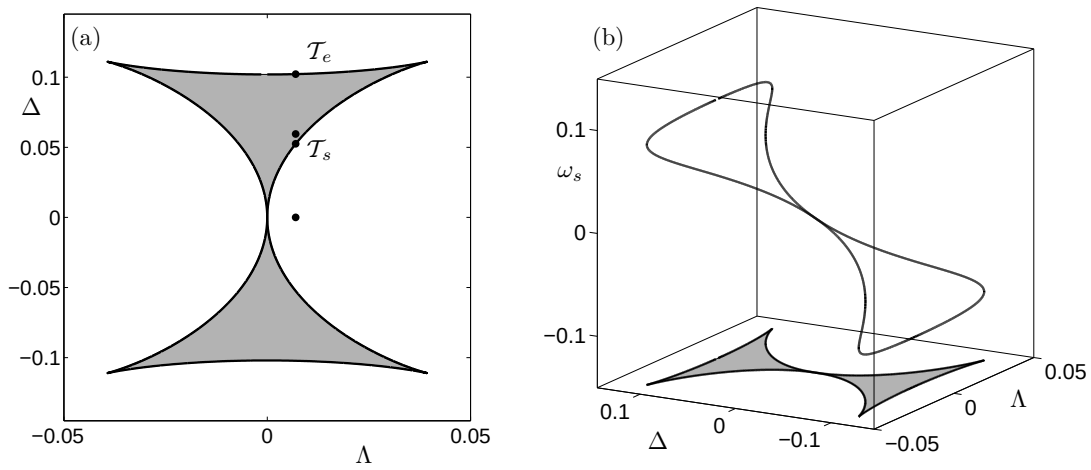

Figure 3. Locus of points containing one (shaded) and two EFM-components (unshaded).

Figures 2(a) to (d) show the fourth-order curve Eq. (21) for $\Delta = 0.0$, 0.0525, 0.0595 and 0.10222, respectively. Intersections of this curve with $F(\omega_s) = 0$ correspond to intersections of the solution envelope with $\Omega = 0$; see Fig. 1. The solution curve and, hence, the EFM-frequencies must lie within these intersection points. In Fig. 2, the intersections are shown as dots; the possible EFM-frequencies as thick lines. We refer to these intervals of possible EFM-frequencies, for a given parameter set, as *EFM-components*.

As Δ is increased, Fig. 2(b), for $\Delta = 0.0525$, shows that the fourth-order curve has a tangency $\mathcal{T}_s$ (a saddle transition) at $F(\omega_s) = 0$. At this point, the number of EFM-components changes from one to two (as is shown in Fig. 2(c) for $\Delta = 0.0595$). One EFM-component is centred around the solitary laser frequency $\omega_s = 0$; the second EFM-component is centred around the filter detuning $\omega_s = \Delta$. Further increasing Δ sees a second tangency $\mathcal{T}_e$ (a transition through an extremum) of the curve at $F(\omega_s) = 0$; see Fig. 2(d), for $\Delta = 0.10222$. This marks a reduction in the number of EFM-components from two to one. The remaining component is centred around the solitary laser frequency $\omega_s = 0$. We note that the tangency $\mathcal{T}_e$ takes place at $\omega_s = \Delta$.

This scenario can actually already be read off from Fig. 1. As Δ is varied, the solution envelope has tangencies $\mathcal{T}_s$ and $\mathcal{T}_e$ with the line $\Omega = 0$. Again, the number of EFM-components changes between one and two when the turning points of the envelope $\mathcal{T}_s$ and $\mathcal{T}_e$ pass through the line $\Omega = 0$. The parameter values at which the tangencies can be found are given by solutions of

$$\frac{dF(\omega_s)}{d\omega_s} = 2\omega_s^2 - 3\Delta\omega_s + \Delta^2 + \Lambda^2 = 0. \tag{22}$$

Namely, by

$$\omega_s = 0, \quad \text{and} \quad \omega_s = \frac{3\Delta \pm \sqrt{\Delta^2 - 8\Lambda^2}}{4}. \tag{23}$$

From these equations we can deduce the following:

- The extremum at $\omega_s = 0$ is always a minimum since $F(0) = -\kappa^2\Lambda^2\left(1+\alpha^2\right)$.
- The two folds for $\omega_s \neq 0$ exist only for $\Delta^2 \geq 8\Lambda^2$.
- The fold for the lower value of ω_s is a maximum ($\mathcal{T}_\mathrm{s}$) and the one for the larger value of ω_s a minimum ($\mathcal{T}_\mathrm{e}$) (note that we consider $\Delta \geq 0$).

The two tangencies $\mathcal{T}_s$ and $\mathcal{T}_e$ come together at cusp points, given as the roots of the derivative of Eq. (22) with respect to ω_s. Namely,

$$\frac{d^2F(\omega_s)}{d\omega_s^2} = 4\omega_s - 3\Delta = 0, \text{ that is, for } \omega_s = \frac{3\Delta}{4}. \tag{24}$$

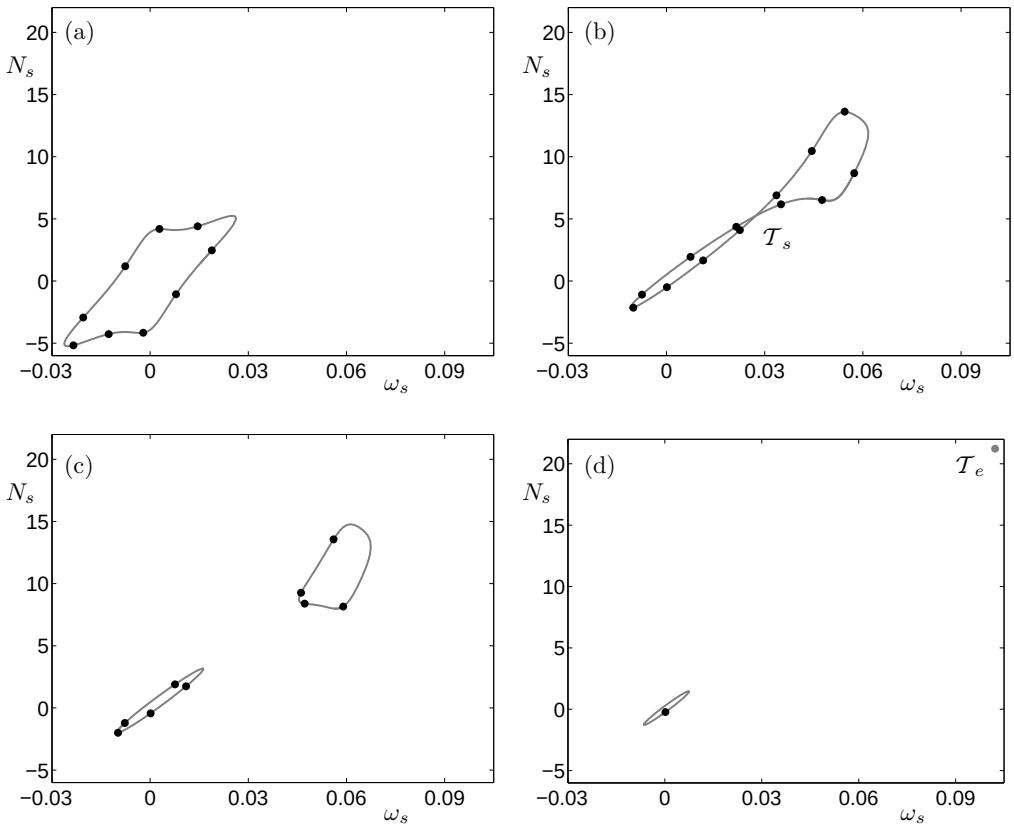

Figure 4. Curves of EFMs in the $(\omega_s,\, N_s)$-plane for $\Delta = 0.0$ (a), 0.0525 (b), 0.0595 (c) and 0.10222 (d).

In the (Λ, Δ)-plane they are found at

$$(\Lambda, \Delta) = \left(\pm\frac{2}{3\sqrt{3}}\kappa\sqrt{1+\alpha^2}, \pm\frac{4\sqrt{2}}{3\sqrt{3}}\kappa\sqrt{1+\alpha^2} \right). \tag{25}$$

Note the linear scaling given by the dressed feedback rate $\kappa\sqrt{1+\alpha^2}$.

Continuation techniques [5] can be used to solve any of the parametric equations derived above. In particular, we can find the locus of fold points given by Eq. (22). Figures 3(a) and (b) show these solutions in the (Λ, Δ)-plane and in $(\Lambda, \Delta, \omega_s)$-space, respectively. Inside the shaded region of Fig. 3(a) we find two EFM-components, outside we find one. It is also shown that the solution of Eq. (22) forms a smooth curve in $(\Lambda, \Delta, \omega_s)$-space (Fig. 3(b)), whose turning points project to the cusp points, Eq. (25), in the (Λ, Δ)-plane (Fig. 3(a)).

For completeness, Fig. 4 shows the EFM-components in the well-documented (ω_s, N_s)-plane. From (a) to (d), the detuning was fixed at Δ =0.0, 0.0525, 0.0595 and 0.10222, respectively. These values of Δ are shown as black dots in Fig. 3. Furthermore, the parameters were chosen to correspond with those used in Ref. [6]. The black dots show the position of the EFMs for $C_p = 0.0$. Recall that, as C_p is varied, these EFMs move along the grey, closed curves of Fig. 4. For $\Delta = 0.0$, Fig. 4 shows a single EFM-component, centred around the solitary laser frequency $\omega_s = 0$. As Δ is increased to $\Delta = 0.0525$, a fold (tangency) of type $\mathcal{T}_s$ is observed; recall Eq. (22). This point is shown to lie on the boundary between the regions of one and two EFM-components in Fig. 3(a). Figure 4(b) shows that the closed curve, denoting a single EFM-component, is about to divide into two. After this fold point $\mathcal{T}_s$, Fig. 4(c) for $\Delta = 0.0595$ clearly shows two separate EFM-components. One EFM-component remains centred around the solitary laser frequency $\omega_s = 0$, the other is centred around the filter detuning frequency $\omega_s = \Delta$. Finally, Fig. 4(d) for $\Delta = 0.10222$, shows the two EFM-components at the second fold (tangency) point $\mathcal{T}_e$. Here, the second EFM-component is denoted by a grey dot. We would only

find an EFM at this tangency by choosing a value of C_p satisfying Eq. (19). Note that this entire transition is in one-to-one correspondence with the changes of the degree-four polynomial Eq. (21) as shown in Fig. 2.

4. CONCLUSIONS

We have presented a detailed study of the EFM structure of the FOF laser. Our analysis has shown how this structure changes as the filter parameters, representing the width Λ, detuning Δ and feedback phase C_p, are varied. Analytic expressions for the solution curve, defining the frequency and amplitude of the EFMs, were given. This showed the dependence of the filter parameters on the EFMs. Furthermore, expressions for the solution envelope, bounding the solution curve, were derived. The (Λ, Δ)-plane was shown to be divided into regions with one or two EFM-components. The boundaries of these regions were shown to correspond to tangencies of the solution envelope with respect to the solitary laser frequency.

REFERENCES

1. K. Green and B. Krauskopf, "Mode structure of a semiconductor laser subject to filtered optical feedback," *Opt. Commun.* **258**, pp. 243–255, 2006.
2. D. Lenstra, G. Vemuri, and M. Yousefi, *Unlocking Dynamical Diversity: Optical Feedback Effects on Semiconductor Lasers*, ch. 4 Generalized Optical Feedback: Theory. Wiley, March 2005.
3. R. Lang and K. Kobayashi, "External optical feedback effects on semiconductor injection laser properties," *IEEE J. Quantum Electron.* **16**(3), pp. 347–355, 1980.
4. K. Green and B. Krauskopf, "Bifurcation analysis of a semiconductor laser subject to non-instantaneous phase-conjugate feedback," *Opt. Commun.* **231**, pp. 383–393, 2004.
5. K. Engelborghs, T. Luzyanina, G. Samaey, and D. Roose, "DDE-BIFTOOL: a Matlab package for bifurcation analysis of delay differential equations," Tech. Rep. TW-330, Department of Computer Science, K. U. Leuven, Belgium, 2001. `http://www.cs.kuleuven.ac.be/cwis/research/twr/research/software/delay/ddebiftool.shtml`.
6. B. Krauskopf, H. Erzgräber, and D. Lenstra, "Dynamics of semiconductor lasers with filtered optical feedback," in *Proc. of SPIE*, **6184**(31), 2006.